Supporting Information

Cu and Zn promoted Al-fumarate metal organic frameworks for electrocatalytic CO_2 reduction

Ung Thi Dieu Thuy[1,*], Tran Ngoc Huan[2,*], Sandrine Zanna[3], Karen Wilson[4], Adam Lee[4], Ngoc-Diep Le,[2] Jim Mensah,[5] Venkata D.B.C Dasireddy[4] and Nguyen Quang Liem[1,*]

[1]Institute of Materials Science, Vietnam Academy of Science and Technology, 18 Hoang Quoc Viet, Cau Giay, Hanoi, Vietnam
[2]Laboratoire de Chimie des Processus Biologiques, Collège de France, Sorbonne Université, 11 Place Marcelin Berthelot, 75231 Paris Cedex 05, France
[3]Chimie ParisTech, PSL Research University, CNRS, Institut de Recherche de Chimie Paris (IRCP), 11 rue Pierre et Marie Curie, 75005 Paris, France
[4]School of Environment & Science, Centre for Catalysis and Clean Energy, Griffith University, Gold Coast Campus, QLD 4222, Australia
[5]Centre for Applied Materials and Industrial Chemistry (CAMIC), RMIT University, Australia
[*] Corresponding authors. E-mails: dieuthuy@ims.vast.vn; ngoc-huan.tran@college-de-france.fr; liemnq@vast.vn

S1 Experimental

CO_2 electroreduction product analysis:

Gaseous products: An on-line gas chromatograph (SRI instruments, MG#5 GC, Ar carrier) was employed to quantify C_2H_4, H_2, CO and CH_4 production. Quantification of H_2 was performed by a thermal conductivity detector with a HaySepD precolumn attached to a 3 m molecular sieve column used to separate H_2 from the other gases. Carbon-containing products were analyzed using a flame-ionization detector with CO and CH_4 separated using a 3 m molecular sieve column, and C_2H_4 and C_2H_6 separated using a 5 m HaySepD column. The GC was calibrated with a gas mixture containing H_2, CO, CH_4, C_2H_4, C_2H_6 and CO_2 as the diluent. Calibration curves for each molecule were obtained by further diluting the gas mixture with CO_2 (both provided by mass flow controllers) before injecting to the GC.

Liquid products: Liquid product yields were determined by ionic chromatrography (MetrohmTM EcoIC) and proton nuclear magnetic resonance spectroscopy (^{1}H-NMR; Bruker Avance III 300 MHz, 300 K). 400 µL of reacted catholyte, 100 µL D_2O (Eurisotop, 99.9%) as a locking solvent and 100 µL of 5 mM aqueous terephthalic acid solution (terephthalic acid, Sigma-Aldrich, 98%) as a reference were mixed and water peaks for each spectrum eliminated by a Pre-SAT180 water suppression method.

Faradaic efficiencies for each product was calculated using the following equation:

$$FE_x(\%) = \frac{n_x \times n_{e\_x} \times F}{Q} \times 100$$

where n_x is the mols of product x, $n_{e\,x}$ is the number of electrons required to generate product x from CO, CO_2 or H_2O, F is the Faraday constant (96500 C.mol^{-1}), and Q the charge passed to generate n_x.

Water adsorption analysis: The samples were placed into a small climate chamber with controlled temperature and relative humidity (TA Instruments, Universal V4.5A). The water adsorption of samples was evaluated at 30 °C and ~90% relative humidity.

S2 Results

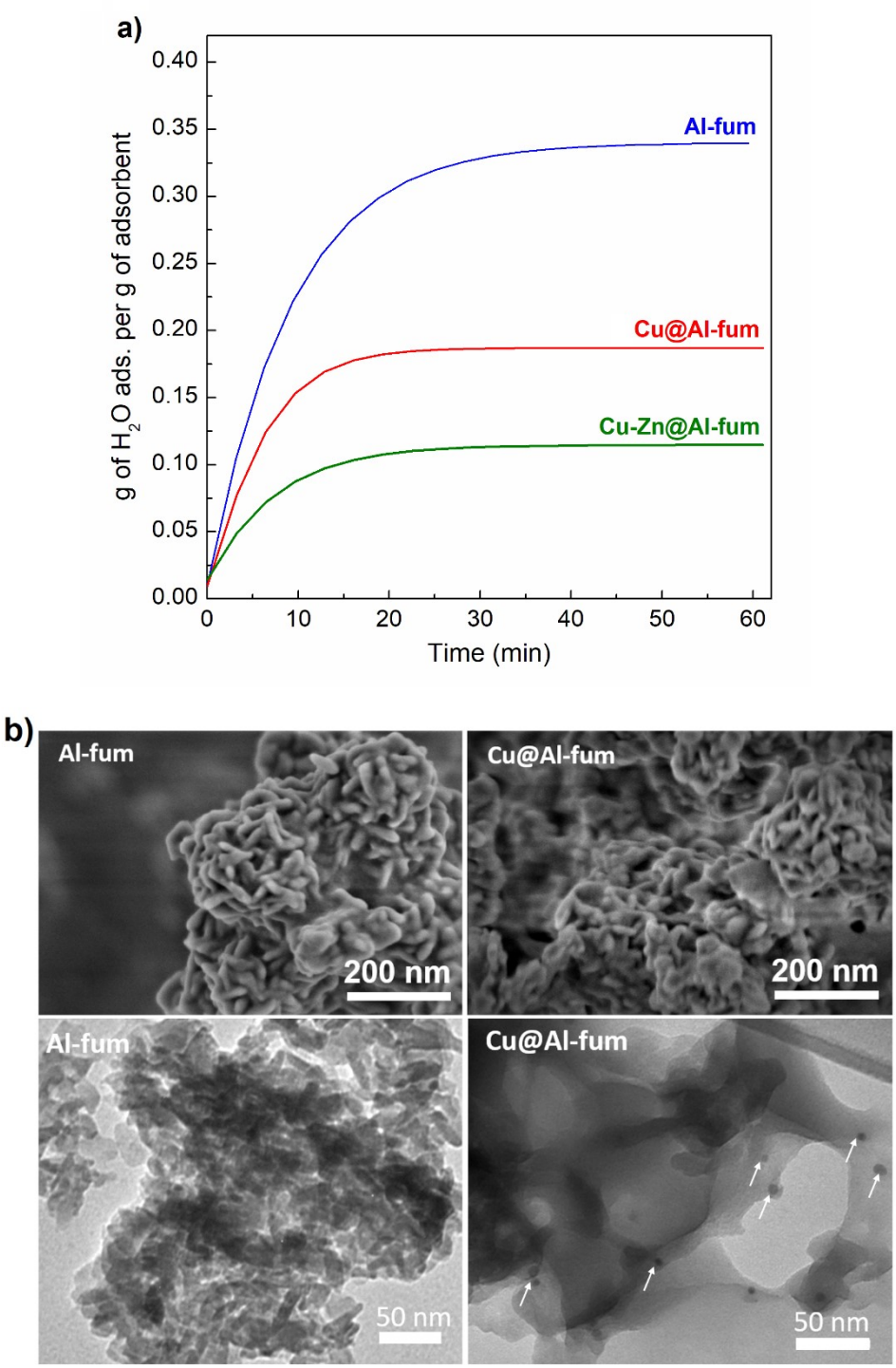

Figure S1. (a) Water adsorption on Al-fum, Cu@Al-fum and Cu-Zn@Al-fum and (b) SEM (top) and TEM (below) images of Al-fum and Cu@Al-fum MOFs.

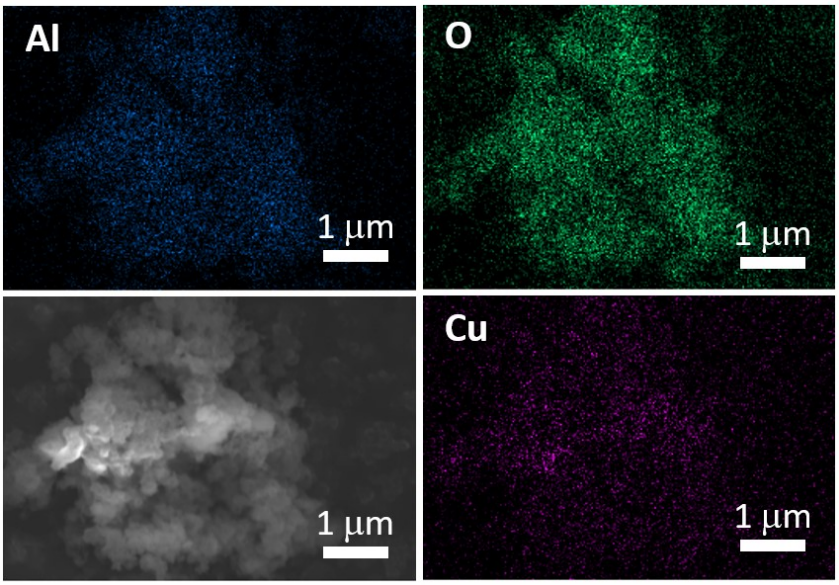

Figure S2. SEM image and corresponding EDX elemental maps of Al, O and Cu for Cu@Al-fum.

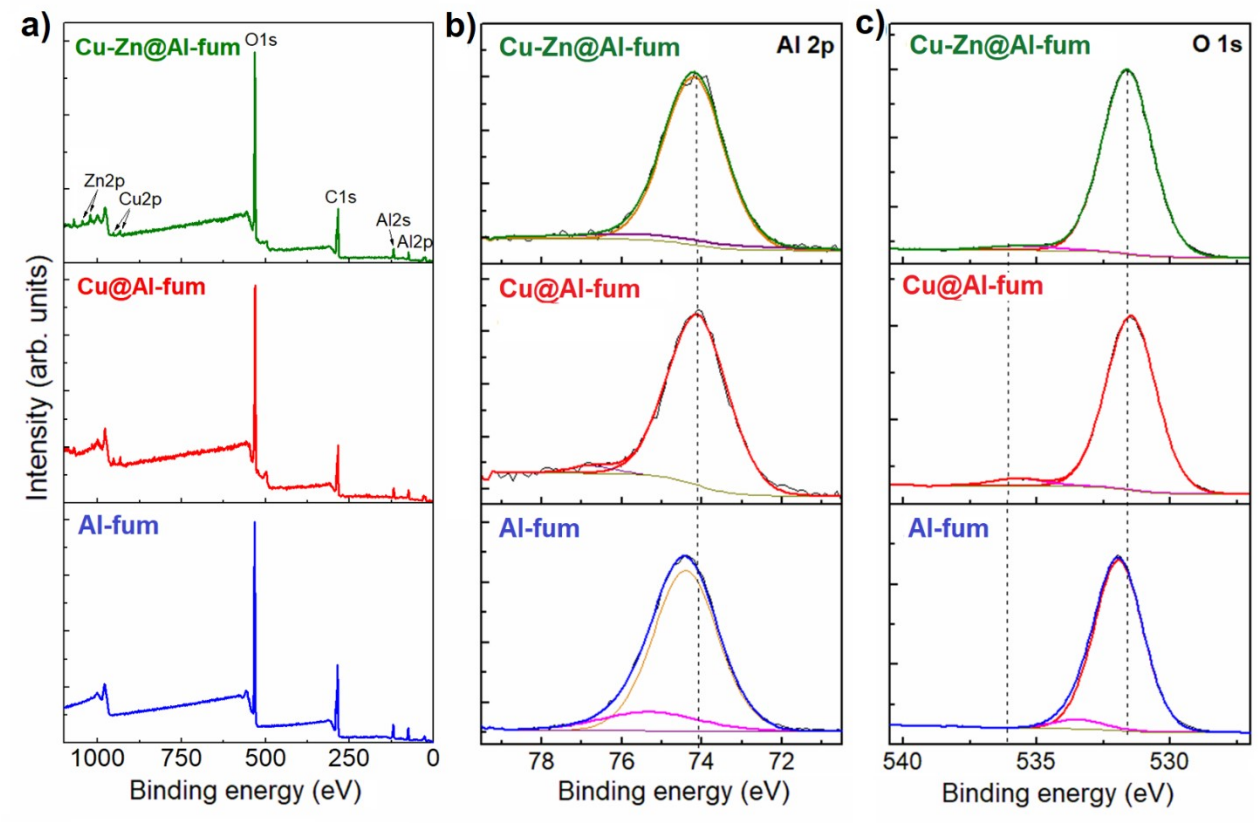

Figure S3. (a) Survey, (b) Al 2p and (c) O 1s XPS spectra of the pristine Al-fum, Cu@Al-fum and Cu-Zn@Al-fum MOFs.

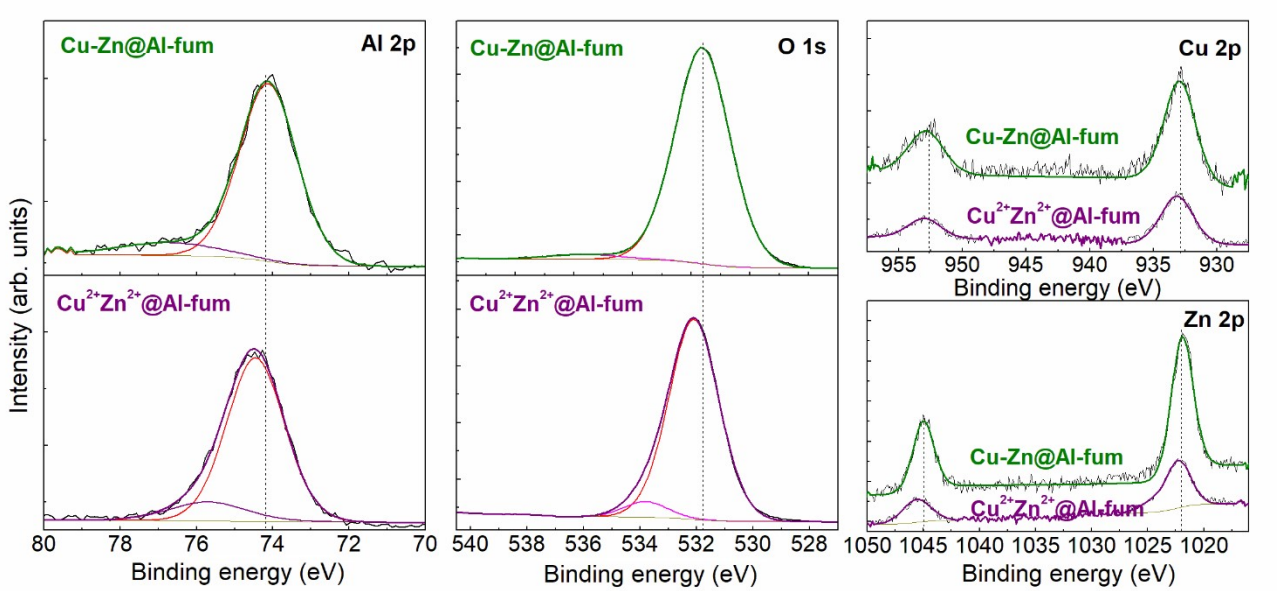

Figure S4. Al 2p, O 1s, Cu 2p and Zn 2p XP spectra of Cu-Zn@Al-fum before (designated $Cu^{2+}Zn^{2+}$@Al-fum) and after treatment with $NaBH_4$.

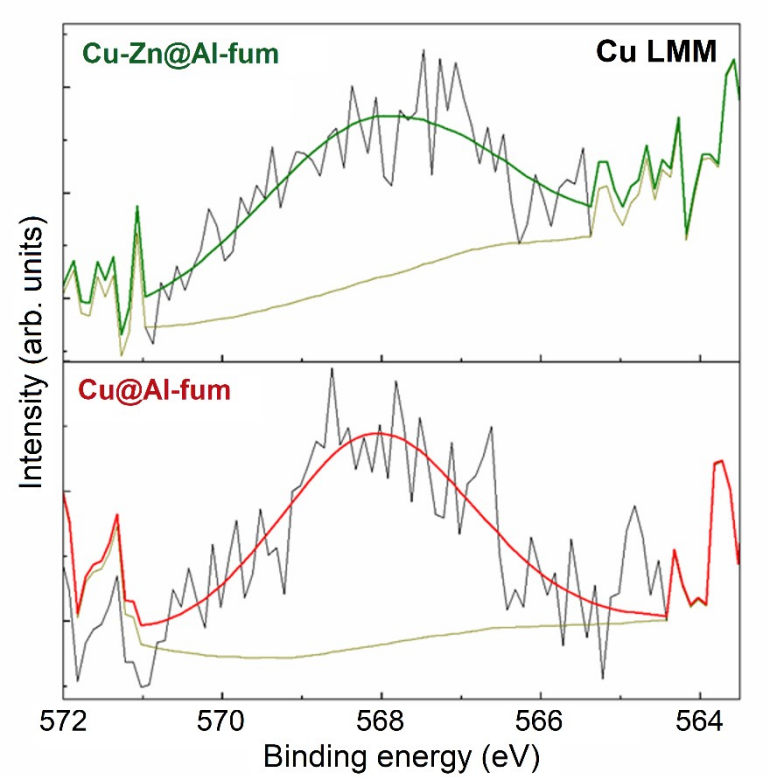

Figure S5. Cu LMM Auger spectra of Cu and Cu-Zn doped Al-fum.

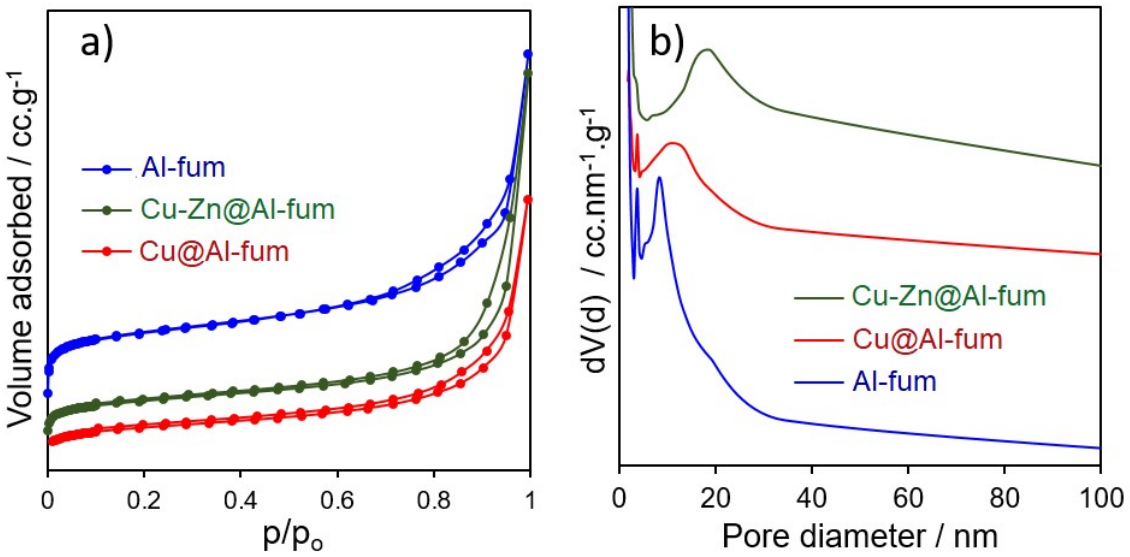

Figure S6. (a) N_2 adsorption-desorption isotherms, and (b) BJH pore size distributions of Al-fum, Cu@Al-fum and Cu-Zn@Al-fum MOFs.

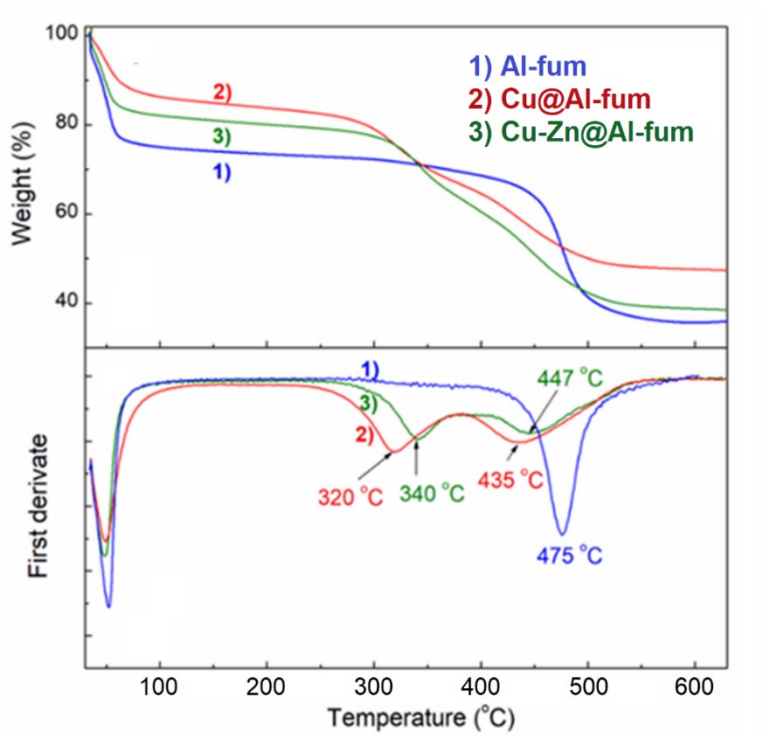

Figure S7. Thermogravimetric analysis profiles and corresponding first derivatives of Al-fum, Cu@Al-fum and Cu-Zn@Al-fum.

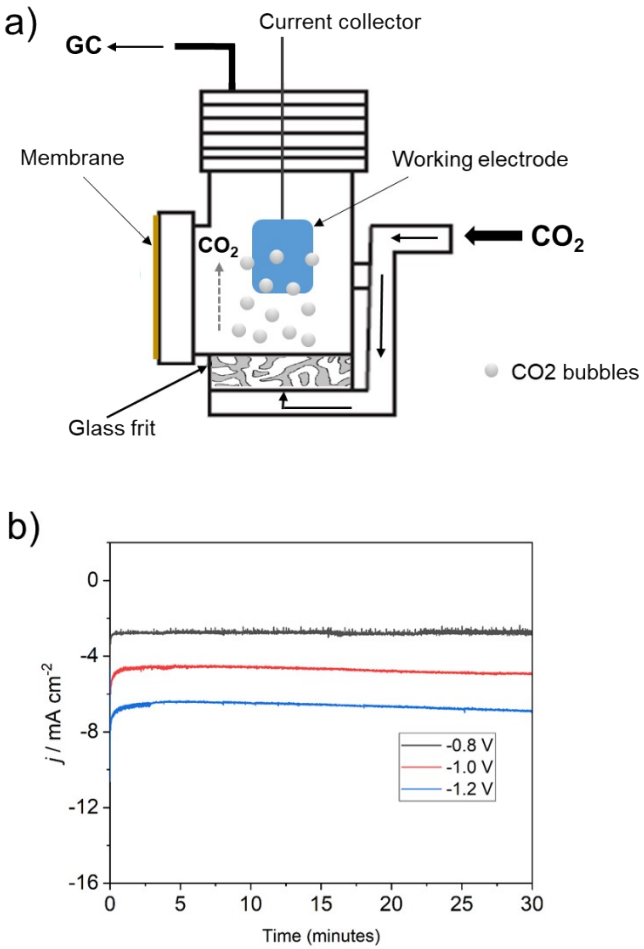

Figure S8. (a) Schematic of cathodic electrochemical cell for CO_2 reduction, (b) time-dependent current density of Cu-Zn@Al-fum/gas diffusion electrode at different cathodic potentials. Measurements made in 0.1 M $KHCO_3$, saturated with CO_2 bubbled at 7.5 ml/min.

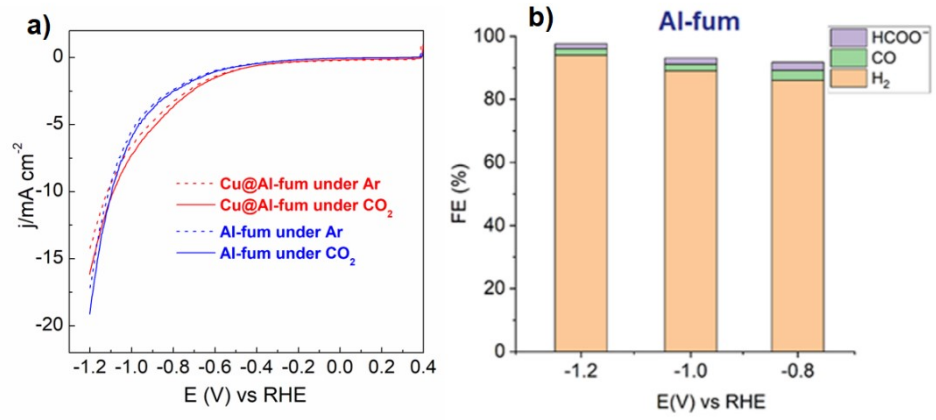

Figure S9. (a) Linear sweep voltammetry curves of Al-fum MOF/GDE and Cu@Al-fum in 0.1 M $KHCO_3$ aqueous solution saturated with CO_2 or Ar, and (b) Faradaic efficiencies for CO_2 reduction products in 0.1 M $KHCO_3$-saturated CO_2 at different cathodic potentials of Al-fum MOF/GDE. CO_2 was continuously bubbled at 7.5 mL.min^{-1} during electrolysis.

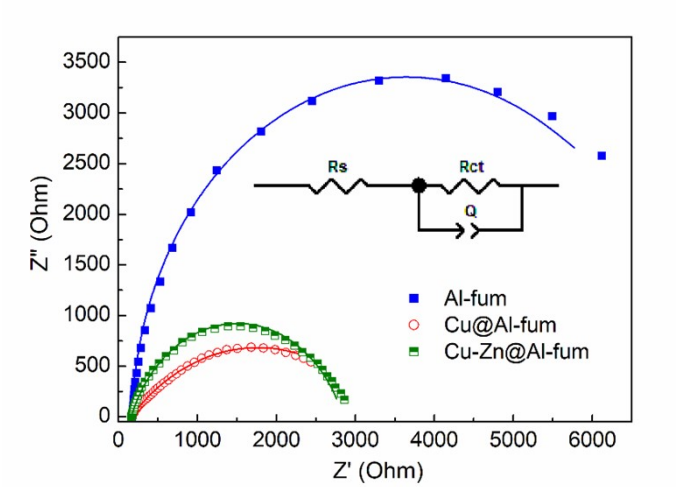

Figure S10. Nyquist plots, with fitting curves (solid lines), of Al-fum MOF, Cu@Al-fum, and Cu-Zn@Al-fum samples in CO_2-saturated 0.1 M $KHCO_3$ with a frequency $10^5 \div 10^{-1}$ Hz at 10 mV of amplitude. The equivalent circuit model is shown on the insert. Rs stands for the contact resistance, Rct for the charge transfer resistance.

Table S1. Quantification of products formed after 30 min CO_2 electroreduction over Al-fum derived electrocatalysts at -1.2V vs RHE.

Sample	H_2 (µmol)	CO (µmol)	HCOOH (µmol)	CH_4 (µmol)	C_2H_4 (µmol)	C_2H_5OH (µmol)[a]	Selectivity to C products (%)
Al-fum	112.4	1.23	1.08	-	-	-	2
Cu@Al-fum	58.5	6.64	6.9	0.49	0.78	-	20
Cu-Zn@Al-fum	23.21	14.91	4.45	2.22	0.77	0.68	50

[a]For ethanol analysis, electrolysis sample was collected after 60 min to enable detection by NMR.

Table S2. Fitted contact resistance (Rs) and charge transfer resistance (R_{ct}) values from Nyquist plots.

Electrode	R_s (Ohm)	R_{ct} (Ohm)	Q (Farad)	n
Al-fum	175.38	6943.4	0.00010948	0.9837
Cu@Al-fum	160.13	3208.3	0.0002241	0.5134
Cu-Zn@Al-fum	163.42	2681.2	0.00003986	0.76914